18th Brazilian Congress of Thermal Sciences and Engineering
November 16-20, 2020 (Online)

ENC-2020-0351
EXTERNAL FLOW'S INFLUENCE ON PCM MELTING TIME IN SPHERES

João Fidelio Raymundo Júnior
Rejane de Césaro Oliveski
Gabriel Eduardo Strohm Eberhardt
Universidade do Vale do Rio dos Sinos - Unisinos
jraymundojunior@gmail.com
decesaroo@gmail.com
gabrielseberhardt@gmail.com

Abstract. *A numerical study on the external flow's influence on the melting of erythritol inside spheres has been carried out. The spheres are arranged in an array and subjected to external flow. This configuration is studied considering three different blockage ratios on the array. The physical model is two-dimensional and transient. The numerical model consists of the continuity, momentum and energy equations and the domain uses a hexahedral mesh. The numerical model is validated using experimental results from the literature and the mesh was verified using the GCI method. Results of liquid fraction over time are presented. All cases present a similar pattern of melting, being more accentuated at the beginning and lower at later moments. For some spheres, there is a reduction in melting time as the distance between them decreases, but that is not the case for spheres at the end of the array. The lowest melting time is seen in a configuration which does not have the maximum neither minimum distance between the spheres, suggesting that the dependency of the melting time in relation to the blockage ratio is not directly neither inversely proportional.*

Keywords: *Thermal storage, Phase change materials, PCM, Computational fluid dynamics*

1. INTRODUCTION

Energy is one of the main key factors in our current society. The constant search for a better living standard and the use of new technologies causes continuous increase in energy demands. In these terms, usually we think of energy as only electric energy, but the use of solar and/or fossil uses being used for heating applications also makes part of our day-to-day lives (Capuano, 2018). Heating used for hot water supply or thermal comfort applications has demanded over 50% of the total world energy demand in 2017 (REN21, 2017). Solar energy, in particular, has the characteristic of not being readily available constantly, which creates the necessity for parallel heating systems in order to supply the energy demand in times where there is no solar irradiation (Sánchez-Pantoja; Vidal and Pastor, 2018). It is, however, possible to storage this solar energy in the form of heat, in the same way that one would store electrical energy in a battery.

There are three main ways to store thermal energy, sensible heat, latent heat and thermochemical energy ((Li, 2016) (Tao; Liu and He, 2017), (Yadav and Banerjee, 2016)). Sensible heat is stored in a substance when its temperature is increased. Latent heat is associated with a phase change, solid-liquid or liquid-vapor, for instance. Thermochemical involves exothermal chemical reactions which release heat, mainly used as a side product in chemical industrial processes ((Spengler, 2019), (Yadav and Banerjee, 2016)). Using latent heat as a mean to store thermal energy has its own characteristics and use cases when compared to the other method. Most phase changes occur at an almost constant temperature, which causes the heat transfer process to happen at an almost constant temperature as well. The whole system control and automation can be simplified. Besides, the thermal density in these latent heat thermal energy storage (LHTES) units is almost 14 times that of a sensible heat storage system with similar dimensions and applications ((Gautam and Saini, 2020), (Spengler, 2019), (Ziskind, 2014)).

LHTES use a material that is subjected to a phase change during its operation, usually called simply as a Phase Change Material, or PCM. This material will change phases, absorbing or releasing heat during the LHTES charge and discharge phases, respectively. LHTES that use melting and solidification, which operate with liquids and solids, are more common and financially viable (Zalba et al., 2003). These systems may be used in domestic and consumer grade applications, such as water heating systems ((Abdollahi and Rahimi, 2020), (Frutos Dordelly et al., 2019)), and electronic devices ((Krishna; Kishore and Solomon, 2017), (Rehman et al., 2018)), as well as in simple industrial uses, like thermal protecting and insulation (Fonseca; Mayor and Campos, 2018) or even much more complex systems in the oil industry (Royo et al., 2019).

There is not a general and universally applied theory for selection of LHTES since there are a wide range of use cases which may be applied in the most different applications. One of the most fundamental uses of LHTES for large scale use

are the Pebble Bed storage systems. In these LHTES, spheres containing a PCM are deposited inside a tank and there is a fluid flowing in between them. The PCM insides the sphere exchanges heat with the sphere's wall, which exchanges heat with the fluid outside. This fluid receives or absorbs heat from the spheres, depending on the temperature differences involved, causing a phase change in the PCM inside the spheres. This heat transfer fluid (HTF) greatly increases the heat transfer capacity, reducing the overall charge and discharge cycles. This effect, combined with a high thermal density, makes the Pebble Bed Storage Systems (PBSS) really interesting for industrial and large scale uses ((Gautam and Saini, 2020), (He et al., 2019), (Karthikeyan et al., 2014), (Regin; Solanki and Saini, 2008), (Zhao et al., 2017)).

The use of PCM to store thermal energy has been broadly studied recently. However, there still are limitations on the approach and methods used in these studies. Detailed experimental studies are complex due to the most diverse physical phenomena happening inside and outside the spheres. This caused a higher attention on the use of numerical techniques. Most of these studies still use a global analysis ((Aziz et al., 2018a), (Bellan et al., 2015), (Guo et al., 2019), (Peng; Dong and Ling, 2014)), or a local analysis with many simplifications on this formulations and methods ((Amin; Bruno and Belusko, 2014), (Assis; Ziskind and Letan, 2009), (Kozak; Rozenfeld and Ziskind, 2014), (Shmueli; Ziskind and Letan, 2010)). The main simplification is the boundary condition used on the sphere's wall. The most used ones are constant temperature or constant heat flux. It is difficult for this condition to be really happening in PBBS. The physical condition is that of external convection over the sphere wall. Besides, each individual point on the sphere has different heat transfer condition, since the flow and heat transfer coefficient are not uniform. Also, there are geometric effects, related to the way the spheres are disposed inside the tank ((Gautam and Saini, 2020), (Kenisarin et al., 2020), (Prieto and Cabeza, 2019)). Studies which consider these effects were not found in the current literature.

This study aims at numerically studying the phase change behaviour of PCM inside a sphere using an external flow boundary condition on the sphere's outside surface.

2. PHASE CHANGE MATERIALS

Any material can go through a phase change at an appropriate temperature is a candidate for being used to store latent thermal energy. In the 70s, these materials started to receive great attention amongst researchers and engineers, focused on increasing the efficiency of solar thermal plants. In the next decade, studies about the behavior of the PCM inside their enclosure would surface, with the main objective of finding ways to enhance the heat transfer between the PCM and other media. This is needed, since most PCM have really low thermal conductivity, which makes it difficult to rapidly extract heat and cause the phase change (Agyenim et al., 2010). Nowadays, it is possible to divide the PCM studies in 3 main areas: applications, physical properties determination for new PCM and the behavior of the PCM during phase change.

2.1 PCM Selection

The main factor for choosing a PCM for an application is its phase change temperature. It is necessary to achieve the thermal demands while being at a temperature range that fits the process needs. In general, an ideal PCM would have high latent heat, thermal conductivity, specific heat and density, while having a low volume change on phase change, low or no sub cooling and well documented and available properties. Also, a good PCM has great chemical stability through many phase change cycles, has a low cost and good availability on the market (Gil et al., 2010).

3. HEAT TRANSFER IN PEBBLE BED HEAT STORAGE UNITS

Conduction is not the only heat transfer mechanism in PBBS, which is different from what happens in storage units that only use sensible heat. A representation of the main heat transfer processes that happen in a PBBS is shown in Figure 1. What happens is the combined effect of many different phenomena: conduction between the spheres, thermal radiation, convection on the spheres outside wall and the heat transfer fluid and the heat transfer between the many different heat transfer fluid currents. Certain phenomena have a higher impact than others. The conduction between the spheres has a low overall contribution, due to the small contact area between them. Thermal radiation is also negligible, since the temperature differences inside the tank are small for the radiation to have a considerable effect. However, in certain cases (specially using metallic PCMs), the temperatures are high enough that this effect must be considered (Wu et al., 2017). Forced convection between the heat transfer fluid and the spheres is the main heat transfer process in PBBS. Since the fluid is free to move in between all the spheres, there is a big heat transfer area, improving the convection effect. However, this characteristic also causes an increase in pressure drop in the overall system ((De Gracia and Cabeza, 2014), (Liu et al., 2020), (Singh and Saini, 2010)). In addition to all the processes cited before, there are also all the mechanisms that occur inside the spheres during the phase change ((Aziz et al., 2018b), (Karthikeyan et al., 2014)).

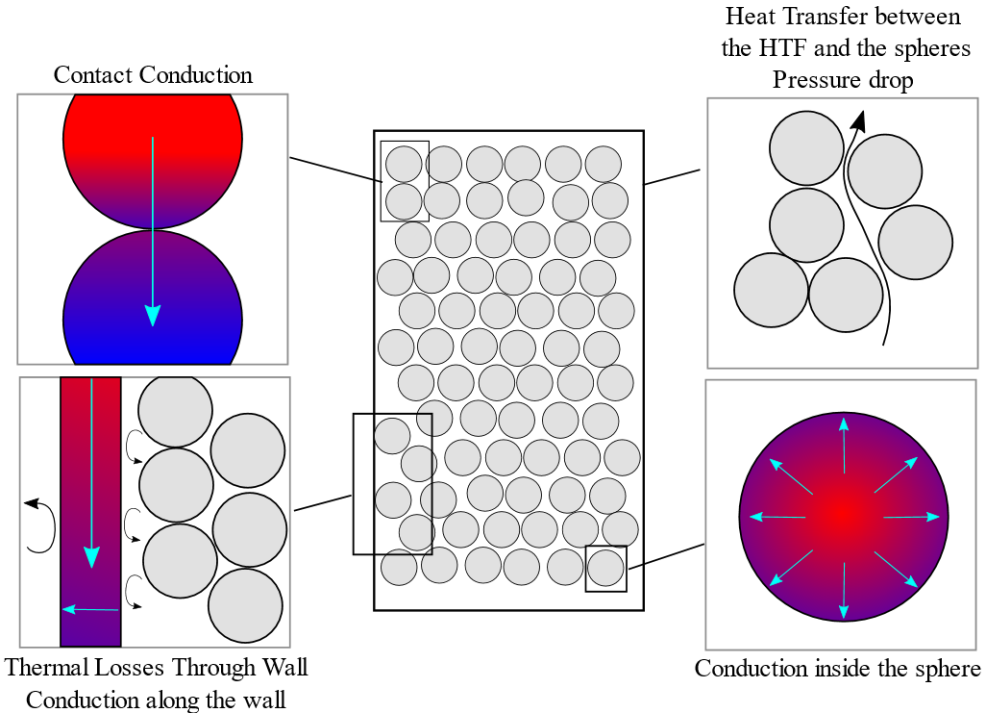

Figure 1 – Heat transfer mechanisms in pebble bed heat storage units
Source: adapted from Gautam e Saini (2020)

3.1 Geometric Parameters used in PBSS

In order to properly analyze the heat transfer in PBBS, the knowledge about the sphere distribution inside the tank is important. Some geometric concepts are introduced, such as: coordination number and blockage ratio. The coordination number is a number that represents on many other spheres are in contact with a certain sphere. If the coordination number is 3, this means that, on average, each sphere is in contact with 3 other spheres. A higher coordination number will provide a small increase in heat transfer, since the effects of conduction will increase, while having almost no impact on the connective effects (Zhang et al., 2011).

The blockage ratio (ψ) is defined as the ratio of the distance between two spheres in the direction of a certain axis and the spheres' diameter. This ratio gives an idea on the amount of empty space in the tank. The bigger the blockage ratio, the emptier space there is. The understanding of the effects caused by these empty spaces is essential, since they directly influence the heat transfer characteristics (Van Antwerpen; Du Toit and Rousseau, 2010).

4. MATERIALS AND METHODS

The geometry considered in this study is spherical and 12.7 mm in inner diameter. It is filled with PCM up to 85% of its height, which results in 94% of its volume. The remaining space is filled with air, which compresses as the PCM expands during phase change. This is necessary as the air functions as a damper, absorbing the stresses that would be caused in due to the PCM's expansion if the sphere was completely filled with PCM. The wall is made of aluminum, with 2 mm thickness. Air flows over the sphere, at a temperature which is higher than the PCM's melting temperature. The sphere is closed, so there's not mass transfer to the outside. With the aim of representing a generic process, the PCM used is erythritol, which phase change temperature (solid – liquid) is 391 K. It is more subject to being used in vapor or combustion gases recirculation processes, due to having a higher melting temperature than most common PCMs such as paraffin waxes (Nomura; Okinaka and Akiyama, 2010). Figure 2 shows a representation of the physical model.

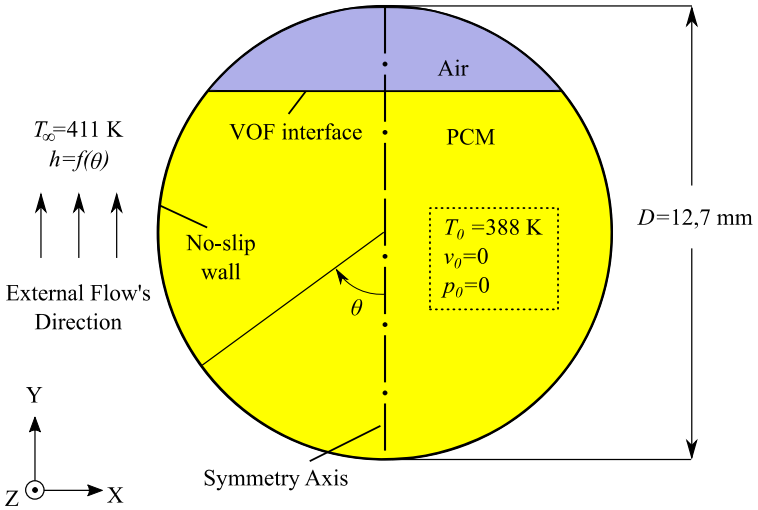

Figure 2 – Physical model representation and boundary conditions

The physical properties of erythritol used in this study are a combination of properties used in 3 distinct studies (Agyenim et al., 2010), (Hesaraki, 2010) e (Sillik and Gregson, 2012)). This is because no study has actually presented all physical properties needed as a function of temperature. The study presented by Agyenim et al. (2010), did not use viscosity values as a function of temperature. So, the values used here are the ones showed by Sillik and Gregson (2010). These authors showed experimental viscosity results, showing that it depends on the temperature in a log scale. All physical properties used are shown in Table 1

Table 1 –Erythritol

Property	**Value**
Latent Heat during melting (J kg^{-1})	339,800
Density (kg m^{-3})	1480 (389 K); 1300 (413 K)
Specific Heat (J kg^{-1} K^{-1})	1350 (389 K); 2740 (413 K)
Thermal Conductivity (W m^{-1} K^{-1})	0.733 (389 K); 0.326 (413 K)
Dynamic Viscosity (kg m^{-1} s^{-1})	$2.7749X10^{-5}T^2$ - 0.0231747T + 4.844
Solidus Temperature (K)	389
Liquidus Temperature (K)	391

Source: adapted from Agyenim et al., (2010); Hesaraki, (2011) and Sillick and Gregson, (2012).

4.1 Mathematical Model

The mathematical model used to achieve the solutions is presented in this section. The mass conservation results in Equation 1.

$$\frac{\partial \rho}{\partial t} + \nabla(\rho \vec{V}) = 0 \tag{1}$$

where $\vec{V}$ is the velocity vector, ρ is the density and t is the time. Besides the conventional equations used in heat transfer and fluid flow analysis, the mathematical model requires a specific model to deal with the PCM phase change. The model used is the enthalpy-porosity method, proposed by Brent and Voller (1988). The method considers an interface between the solid and liquid phases (region partially melted) as a porous medium. The method does this by introducing a source term in the momentum equation, as per Equation 2.

$$\frac{\partial \rho \vec{V}}{\partial t} + \nabla(\rho \vec{V}\vec{V}) = -\nabla p + \nabla(\mu \nabla \vec{V}) + \rho \vec{g} + \vec{S} \tag{2}$$

where p is the pressure, μ is the dynamic viscosity, $\vec{g}$ is the gravity acceleration and $\vec{S}$ is the source term introduced by the enthalpy-porosity method. The source term is calculated through Equation 3:

$$\vec{S}=\frac{(1-\beta)^2}{\left(\beta^3+\varepsilon\right)}C\vec{V} \tag{3}$$

where ε is a small constant value (0.001) to avoid divisions by 0 (zero), β is the liquid fraction during the phase change and C is a constant proposed by Brent and Voller (1998), the mushy zone constant. The source term introduces a damping in the PCM's velocity in the region in between the solid and liquid phases, causing it to be equal zero near the solid region. The constant indicates the damping magnitude, the higher its value, the higher the damping effect (Voller and Prakash, 1987). The PCM liquid fraction during the phase change is calculated using Equation 4:

$$\beta=\begin{cases}0 & \text{se} \quad T<T_s \\ 1 & \text{se} \quad T>T_l \\ \frac{T-T_s}{T_l-T_s} & \text{se} \quad T_s<T<T_l\end{cases} \tag{4}$$

where T_s and T_l are the *solidus* and *liquidus* temperatures, respectively. Equation 5 describes the energy conservation:

$$\frac{\partial(\rho\lambda)}{\partial t}+\nabla\left(\rho\vec{V}\lambda\right)=\nabla(k\nabla T) \tag{5}$$

where λ is the total enthalpy, obtained by the sum of the sensible enthalpy and (λ_{se}) and the enthalpy variation during the phase change (λ_L). The sensible enthalpy is given by Equation 6 (Ziskind, 2014):

$$\lambda_{se}=\lambda_{ref}+\int_{T_{ref}}^{T}C_p dT \tag{6}$$

where λ_{ref} is the PCM's enthalpy at the reference temperature. T_{ref}. The enthalpy variation during the phase change is a function of the liquid fraction, as per Equation 7:

$$\lambda_L=\beta L, \tag{7}$$

where L is the latent heat. This means that the liquid fraction functions as a proportionality coefficient that multiplies the latent heat in a way that the phase change enthalpy is equal to the latent heat when the PCM is completely melted. The liquid fraction is defined as the ratio between the liquid PCM mass and the total PCM mass. It represents a percentage of the quantity of PCM in the liquid state, that is, the mass of PCM that has already absorbed enough heat to undergo a phase change. So, the liquid fraction also represents the quantity of latent heat stored by the PCM, as a percentage of the maximum latent heat that can be stored.

The physical model considers two different material (solid/liquid PCM and air), which don't mix and have no chemical interactions. To account for their physical interaction, the VOF (Volume of Fluid) multiphase model is used (Ansys, 2013). This model calculates the volume fraction for each fluid, using Equation 8:

$$\frac{\partial(\gamma_n)}{\partial t}+\nabla\left(\alpha_n\vec{V}\right)=0 \tag{8}$$

where γ_n is the primary phase (PCM) volume fraction at the nth computational volume. This volume fraction is ratio between the PCM and air volumes in a given cell. When the cell is completely filled with PCM, its value is 1, and 0 when the cell is completely filled with ar. Any value other and these represents means that the cell has both PCM and air inside, something that only happens numerically.

The air is present inside the sphere to absorb the PCM's expansion during phase change and avoid high stresses on the spheres structure through the changes in its density as a function of pressure. To account for this, the air is modeled as an ideal gas using Equation 9:

$$\rho=\left(p_{op}+p\right)\left(\frac{R}{M_w}T\right)^{-1}, \tag{9}$$

where p_{op} is the operating pressure (atmospheric), R the gas constant and M_w is the molecular weight. The boundary condition on the sphere is convection as per Equation 10:

$$-k_w\left.\frac{\partial T}{\partial\theta}\right|_{\theta=0\text{-}180^\circ}=h(\theta)(T_\infty-T_W) \tag{10}$$

4.2 Numerical Approach

All analyses were done exclusively through numerical simulations. This was done through CFD, computational fluid dynamics. The simulations were done using Ansys' CFD package. Specifically, the following software were used: ICEM CFD for geometry and mesh preparation, Fluent for the processing and CFD-Post (from the CFX package) was used for post processing.

The computational domain is two-dimensional, with an axisymmetric condition. Even though the sphere is a tridimensional sphere, it is possible to represent it in its two-dimensional form, a circle, through the use of this axisymmetric condition. The domain has two control surfaces, the sphere's wall and the axisymmetric axis. This axis splits the circle in two equal parts. The correct implementation requires that only half of the circle is modeled. The inside wall has a no-slip condition.

On the outside wall, a profile of the local heat transfer coefficient is prescribed, with the values presented by Kao et al., (2014). The specific values depend on the specific case being studied. The whole arrangement consists for three spheres and each one of them has its own different values. These values are implemented on Fluent using UDFs (user-defined functions) using C language. The use of these coefficients makes it possible to simulate each sphere individually, since the effect that one sphere has one the other has already been accounted for on the heat transfer coefficient results presented by Kao et al., (2014). The major advantage is to eliminate the need of simulating the external flow.

All simulations had the same initial temperature for all domain (PCM+Air) and is 3 K below the PCM's melting temperature, which is 391 K. The external air temperature is constant and uniform, due to its high Reynolds number, which causes the air temperature to have only a small change when flowing over one individual sphere. The boundary conditions are depicted in Figure 2. The right side of the sphere (to the right of the symmetry axis) is not simulated, due to the symmetry condition used here.

Based on the literature and previous studies, the methods used are: *PISO* for the pressure-velocity coupling, *PRESTO!* for pressure correction, *Second Order Upwind* for the momentum and mass and energy conservation equations. The gradients were solved using the *Least Squares Cell Based* method. The *Geo-Reconstruct* method is necessary to correct the volume fraction in the VOF model. All the methods are available in Fluent without the need of additional programming. Under-relaxation factors are needed to guarantee the solution's convergence, 0.3 for pressure, 0.2 for liquid fraction, 0.9 for energy and 0.5 for both continuity and momentum. All simulations were done using floating point double precision.

Each time step is equivalent to 0.010 seconds and runs enough iterations until all convergence criteria is reached, which happened to be around 500 in the earlier stages and 100 at the late stages of the simulations. The convergence criteria are 10^{-6} for continuity and momentum and 10^{-8} for energy in numeric residue.

Cases considering the external flow in the positive Y direction, with 20 K temperature difference between the external flows temperature and the PCM melting temperature (ΔT) and for different blockage ratios (ψ) for all three spheres positions were tested.

To ensure that the mesh is appropriate, a mesh verification was performed through the GCI method. This method determines the discretization uncertainty associated with the mesh. The results used in this method were the liquid fraction over time for the case with the sphere 1 with ψ=1.5 and ΔT=15 K. The maximum uncertainty value found was 0.758%. The average value is 0.298%. Considering these results, it is safe to consider the mesh as validated an appropriate for this study.

4.3 Implementing the local heat transfer coefficient values as a boundary condition

As mentioned previously, it was not possible to find values for the local heat transfer coefficient for spheres in pebble beds. However, there are results obtained in a certain spheres arrangement in different thermal and flow conditions. The values used in this study are the ones shown by Kao et al., (2014).

Conventionally, in Fluent, it is possible to use a simple convection boundary condition, using a single heat transfer coefficient value and a single free stream temperature value. However, these values are uniform and constant along the whole control surface. This is a characteristic of almost all of Fluent's boundary conditions setup. However, it is possible to insert functions as boundary conditions, *h* as a function of the sphere's angle in this case. This is done through the use of user defined functions, which is special code introduced in Fluent in C language. The results obtained by Kao et al., (2014) were adjusted into functions and then implemented as UDFs.

5. RESULTS AND DISCUSSIONS

The numerical model validation was done through the experimental results of Assis et al., (2007). The authors used RT27 as PCM, and this validation did the same. The geometry is a sphere with 80 mm in diameter, filled with PCM up to 85% of its height, with air completing the remaining volume. The authors used a constant wall temperature condition at the sphere's wall, using a constant temperature bath at 310 K, 10 K above this PCM's melting temperature. The initial

temperature condition is 298 K. The results obtained in by these authors are then compared with results obtained used in this study, using the same conditions.

The quantitative validation is presented in Figure 3. It is possible to note that the results obtained in this study show good agreement with the experimental results obtained by Assis et al. (2007). Up until 7.5 min, there is an overlap between the results. After this time, there is a small deviation, approximately 0.04 between the experimental and numerical results. The maximum deviation is 0.06, at 23 minutes. Due to the small differences noted between the results, the model is considered as validated.

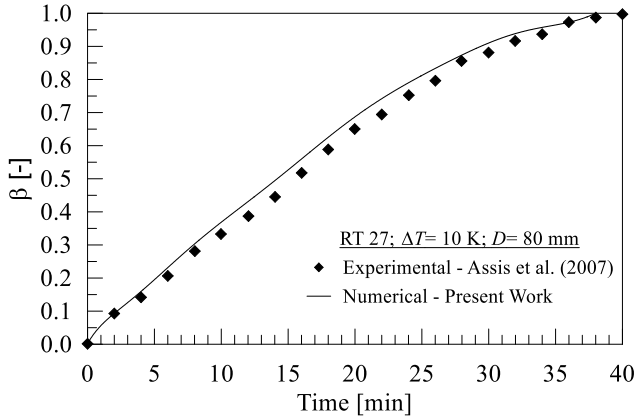

Figure 3 – Liquid fraction vs. Time: RT27, ΔT= 10 K e D= 80 mm.

Figure 4 shows the liquid fraction over time for sphere 1, with ΔT= 20 K and ψ=1.500, 1.125, 0,750 and 0.550. It shows the influence that the blockage ratio has on the liquid fraction. It is possible to note that, for all cases, the phase change process is much faster at the beginning. This is evident in the early slope in the liquid fraction curve. In later moments, around 5 minutes, the rate at which the liquid fraction increases actually decreases. This makes sense, because the lower the value of β, the lower the average temperature inside the sphere, since there is a bigger mass of solid PCM. This lower average temperature causes the heat transfer to be higher, due to the higher temperature difference. When β is higher, there is not much solid PCM, causing the average temperature to be lower and, thus, the heat transfer to be lower. However, it is important to note the temperature in regions in contact with solid PCM do not change, since the PCM maintains an almost constant temperature during phase change. Also, there is almost no difference in the β values at a given time, comparing cases with different values of ψ.

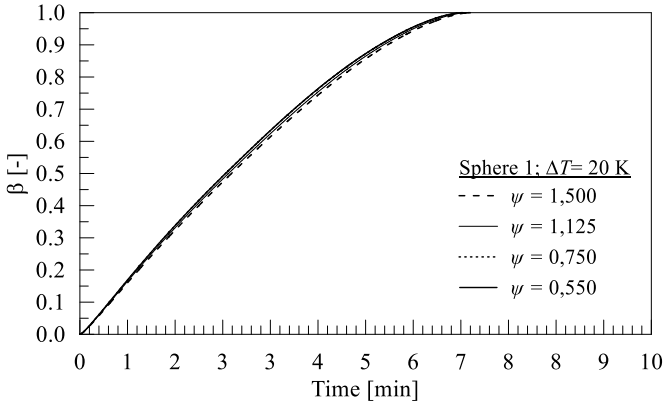

Figure 4 –Liquid fraction vs time: Sphere1, ΔT=20 K e ψ=1.500, 1.125, 0.750 e 0.550.

Table 1 shows the total melting time for cases with ΔT=20 K, ψ=1.5, 1.125, 0.75 and 0.55, for the 3 sphere's position. The total melting time is achieved when the PCM liquid fraction is equal to 1, which means that all PCM is in the liquid state, and it is not possible to store any more latent heat. It is, however, still possible for the PCM to still store more thermal energy through sensible heat, and this process will only stop when the PCM is in thermal equilibrium with the outside air flow. For all ψ values, sphere 3 is the one that has the highest total melting time. Note that the time required for sphere 3 to achieve a melt fraction value of 1 increases as the blockage ratio values get lower. For ψ=1.500, this difference is approximately 24 seconds, while for ψ=0.750 and 0.550, it is 91.88 and 164.5 seconds, respectively. In this period, the other spheres can no longer store latent heat, since all PCM is already melting and start to accumulate sensible heat, which is not the objective.

It is also possible to note that sphere 1, the first one to come into contact with the external flow, is not necessarily the first one to achieve a complete melting cycle. This is true for ψ=1.500, but for the rest of the cases, sphere 2 is the one

that has the lower melting times. The total melting time difference between sphere 1 and sphere 2 increases at the values of ψ become smaller. This may be related to the external flow's turbulence in regions next to sphere 2, associated with the fact the spheres are closer together. Finally, the blockage ratio that has the lower total melting time for all sphere is ψ=1,.125, showing that the charging time as a function of ψ is not directly nor inversely proportional.

Table 2 – Total melting time (s): ΔT=20 K, ψ=1.5, 1.125, 0.75 and 0.55 for all 3 sphere positions.

ψ	Sphere 1	Sphere 2	Sphere 3
1.500	412.08	419.50	444.13
1.125	406.13	405.38	437.25
0.750	402.25	399.13	494.13
0.550	401.75	394.17	566.25

6. CONCLUSIONS

This study main objective was to analyze the influence of using a non-uniform heat transfer coefficient boundary condition in the melting characteristics of PCM inside a sphere. The study was made using CFD, using the Fluent software. The mathematical model is made of the continuity, momentum and energy conservation equations, along with a multiphase model (VOF) and a multiphase model (enthalpy-porosity). The computational domain is two dimensional and axisymmetric, using a hexahedral mesh. The model was validated using experimental results from the literature. The mesh was verified using the GCI method. The non-uniform heat transfer coefficient boundary condition was introduced in Fluent using UDFs, with results available in the literature.

The results obtained suggest that:

- All cases show a similar pattern of their liquid fraction over time, being more accentuated at the beginning of the simulation and lower at later moments;
- Considering spheres 1 and 2, when the distance between them is reduced (reducing the blockage ratio), there was a decrease in total melting time;
- Considering sphere 3, there is a decrease in total melting time from ψ=1.500 to 1.125, however there is a significant increase in total melting time if ψ is further decreased;
- The configuration with ψ=1.125 is the one that showed the less overall melting time for the whole array, suggesting that the relation between ψ and the total melting time for the array is not directly of inversely proportional.

7. ACKNOWLEDGEMENTS

The authors would like to thank CAPES, FAPERGS and Unisinos for their financial support.

8. REFERENCES

ABDOLLAHI, N.; RAHIMI, M. Potential of water natural circulation coupled with nano-enhanced PCM for PV module cooling. **Renewable Energy**, v. 147, p. 302–309, 2020.

AGYENIM, F. et al. A review of materials, heat transfer and phase change problem formulation for latent heat thermal energy storage systems (LHTESS). **Renewable and Sustainable Energy Reviews**, v. 14, n. 2, p. 615–628, 2010.

AMIN, N. A. M.; BRUNO, F.; BELUSKO, M. Effective thermal conductivity for melting in PCM encapsulated in a sphere. **Applied Energy**, v. 122, p. 280–287, 2014.

ANSYS. ANSYS Fluent Theory Guide. **ANSYS Inc., USA**, n. November, 2013.

ASSIS, E.; ZISKIND, G.; LETAN, R. Numerical and Experimental Study of Solidification in a Spherical Shell. **Journal of Heat Transfer**, v. 131, n. 2, p. 024502, 2009.

AZIZ, S. et al. CFD simulation of a TES tank comprising a PCM encapsulated in sphere with heat transfer enhancement. **Applied Thermal Engineering**, v. 143, p. 1085–1092, 2018a.

AZIZ, S. et al. Effectiveness-NTU correlation for a TES tank comprising a PCM encapsulated in a sphere with heat transfer enhancement. **Applied Thermal Engineering**, v. 143, p. 1003–1010, 2018b.

BELLAN, S. et al. Numerical and experimental studies on heat transfer characteristics of thermal energy storage system

packed with molten salt PCM capsules. **Applied Thermal Engineering**, v. 90, p. 970–979, 2015.

CAPUANO, L. Internatinal energy outlook 2017. **U.S. Energy Information Administration**, v. IEO2017, n. 2018, p. 143, 2018.

DE GRACIA, A.; CABEZA, L. F. Numerical simulation of a PCM packed bed system: A review. **Renewable and Sustainable Energy Reviews**, n. October 2014, 2014.

FONSECA, A.; MAYOR, T. S.; CAMPOS, J. B. L. M. Guidelines for the specification of a PCM layer in firefighting protective clothing ensembles. **Applied Thermal Engineering**, v. 133, p. 81–96, 2018.

FRUTOS DORDELLY, J. C. et al. Experimental analysis of a PCM integrated solar chimney under laboratory conditions. **Solar Energy**, v. 188, n. May, p. 1332–1348, 2019.

GAUTAM, A.; SAINI, R. P. **A review on technical, applications and economic aspect of packed bed solar thermal energy storage systemJournal of Energy Storage**Elsevier Ltd, , 1 fev. 2020.

GIL, A. et al. State of the art on high temperature thermal energy storage for power generation. Part 1-Concepts, materials and modellization. **Renewable and Sustainable Energy Reviews**, v. 14, n. 1, p. 31–55, 2010.

GUO, Z. et al. CFD analysis of fluid flow and particle-to-fluid heat transfer in packed bed with radial layered configuration. **Chemical Engineering Science**, v. 197, p. 357–370, 2019.

HE, Z. et al. Cyclic characteristics of water thermocline storage tank with encapsulated PCM packed bed. **International Journal of Heat and Mass Transfer**, v. 139, p. 1077–1086, 1 ago. 2019.

HESARAKI, A. **CFD modeling of heat charging process in a direct-contact container for mobilized thermal energy storage**. [s.l.] Mälardalen University Sweden, 2011.

KAO, M. T. et al. Investigating effects of sphere blockage ratio on the characteristics of flow and heat transfer in a sphere array. **Energy Conversion and Management**, v. 81, p. 455–464, 2014.

KARTHIKEYAN, S. et al. Parametric studies on packed bed storage unit filled with PCM encapsulated spherical containers for low temperature solar air heating applications. **Energy Conversion and Management**, v. 78, p. 74–80, 2014.

KENISARIN, M. M. et al. **Melting and solidification of PCMs inside a spherical capsule: A critical reviewJournal of Energy Storage**Elsevier Ltd, , 1 fev. 2020.

KOZAK, Y.; ROZENFELD, T.; ZISKIND, G. Close-contact melting in vertical annular enclosures with a non-isothermal base: Theoretical modeling and application to thermal storage. **International Journal of Heat and Mass Transfer**, v. 72, p. 114–127, 2014.

KRISHNA, J.; KISHORE, P. S.; SOLOMON, A. B. Heat pipe with nano enhanced-PCM for electronic cooling application. **Experimental Thermal and Fluid Science**, v. 81, p. 84–92, 2017.

LI, G. Sensible heat thermal storage energy and exergy performance evaluations. **Renewable and Sustainable Energy Reviews**, v. 53, p. 897–923, 2016.

LIU, L. et al. Experimental analysis of flow and convective heat transfer in the water-cooled packed pebble bed nuclear reactor core. **Progress in Nuclear Energy**, v. 122, n. September 2019, 2020.

NOMURA, T.; OKINAKA, N.; AKIYAMA, T. Technology of Latent Heat Storage for High Temperature Application: A Review. **ISIJ International**, v. 50, n. 9, p. 1229–1239, 2010.

PENG, H.; DONG, H.; LING, X. Thermal investigation of PCM-based high temperature thermal energy storage in packed bed. **Energy Conversion and Management**, v. 81, p. 420–427, 2014.

PRIETO, C.; CABEZA, L. F. Thermal energy storage (TES) with phase change materials (PCM) in solar power plants (CSP). Concept and plant performance. **Applied Energy**, 2019.

REGIN, A. F.; SOLANKI, S. C.; SAINI, J. S. Heat transfer characteristics of thermal energy storage system using PCM capsules: A review. **Renewable and Sustainable Energy Reviews**, v. 12, n. 9, p. 2438–2451, 2008.

REHMAN, T. UR et al. Copper foam/PCMs based heat sinks: An experimental study for electronic cooling systems. **International Journal of Heat and Mass Transfer**, v. 127, p. 381–393, 2018.

REN21. **Global Status Report, Renewable 2017**. [s.l: s.n.]. v. 72

ROYO, P. et al. High-temperature PCM-based thermal energy storage for industrial furnaces installed in energy-intensive industries. **Energy**, v. 173, p. 1030–1040, 2019.

SÁNCHEZ-PANTOJA, N.; VIDAL, R.; PASTOR, M. C. Aesthetic impact of solar energy systems. **Renewable and Sustainable Energy Reviews**, v. 98, n. August, p. 227–238, 2018.

SHMUELI, H.; ZISKIND, G.; LETAN, R. Melting in a vertical cylindrical tube: Numerical investigation and comparison with experiments. **International Journal of Heat and Mass Transfer**, v. 53, n. 19–20, p. 4082–4091, 2010.

SILLICK, M.; GREGSON, C. M. Spray chill encapsulation of flavors within anhydrous erythritol crystals. **LWT - Food Science and Technology**, v. 48, n. 1, p. 107–113, 2012.

SINGH, H.; SAINI, R. P.; SAINI, J. S. A review on packed bed solar energy storage systems. **Renewable and Sustainable Energy Reviews**, v. 14, n. 3, p. 1059–1069, 2010.

SPENGLER, F. **Estudo Numérico do efeito da geometria de Aletas em Armazenadores de calor de Tubos Concêntricos em processo de fusão com Ácido Láurico**. [s.l.] Universidade do Vale do Rio dos Sinos, 2019.

TAO, Y. B.; LIU, Y. K.; HE, Y. L. Effects of PCM arrangement and natural convection on charging and discharging performance of shell-and-tube LHS unit. **International Journal of Heat and Mass Transfer**, v. 115, p. 99–107, 2017.

VAN ANTWERPEN, W.; DU TOIT, C. G.; ROUSSEAU, P. G. A review of correlations to model the packing structure and effective thermal conductivity in packed beds of mono-sized spherical particles. **Nuclear Engineering and Design**, v. 240, n. 7, p. 1803–1818, 2010.

VOLLER, V. R.; PRAKASH, C. A fixed grid numerical modelling methodology for convection-diffusion mushy region phase-change problems. **International Journal of Heat and Mass Transfer**, v. 30, n. 8, p. 1709–1719, 1987.

WU, H. et al. Numerical simulation of heat transfer in packed pebble beds: CFD-DEM coupled with particle thermal radiation. **International Journal of Heat and Mass Transfer**, v. 110, p. 393–405, 2017.

YADAV, D.; BANERJEE, R. A review of solar thermochemical processes. **Renewable and Sustainable Energy Reviews**, v. 54, p. 497–532, 2016.

ZALBA, B. et al. **Review on thermal energy storage with phase change: materials, heat transfer analysis and applications**. [s.l: s.n.]. v. 23

ZHANG, H. W. et al. A DEM study on the effective thermal conductivity of granular assemblies. **Powder Technology**, v. 205, n. 1–3, p. 172–183, 2011.

ZHAO, B. CHEN et al. Cyclic thermal characterization of a molten-salt packed-bed thermal energy storage for concentrating solar power. **Applied Energy**, v. 195, p. 761–773, 2017.

ZISKIND, G. **Modelling of heat transfer in phase change materials (PCMs) for thermal energy storage systems**. [s.l.] Woodhead Publishing Limited, 2014.

9. RESPONSIBILITY NOTICE

The authors are the only responsible for the printed material included in this paper.